Toward improved endoscopic examination of urinary stones: a concordance study between endoscopic digital pictures vs. Microscopy

Vincent Estrade, Baudouin Denis de Senneville, Paul Meria, Christophe Almeras, Franck Bladou, Jean-Christophe Bernhard, Gregoire Robert, Olivier Traxer, Michel Daudon

Toward improved endoscopic examination of urinary stones: a concordance study between endoscopic digital pictures vs. microscopy

Authors:

Vincent Estrade[1], Baudouin Denis de Senneville[2], Paul Meria[3], Christophe Almeras[4], Franck Bladou[1], Jean-Christophe Bernhard[1], Gregoire Robert[1], Olivier Traxer[5], Michel Daudon[6]

[1]Department of Urology, CHU Pellegrin, Place Amelie Raba Leon 33000 Bordeaux, France

[2]University of Bordeaux, IMB, UMR CNRS 5251, 351 Cours de la Libération, F-33405 Talence Cedex, France

[3]Department of Urology, Saint-Louis Hospital, Denis Diderot University, Paris, France

[4]Department of Urology, La Croix du Sud Clinic, 52 chemin de Ribaute, 31130 Quint Fonsegrives, France

[5]Department of Urology, Tenon Hospital, Pierre and Marie Curie University, Paris, France

[6]Unit of Functional Explorations, Tenon Hospital, Pierre and Marie Curie University, Paris, France

Vincent Estrade (vincent.estrade@gmail.com)

Baudouin Denis de Senneville (bdenisde@math.u-bordeaux.fr)

Paul Meria (paul.meria@aphp.fr)

Christophe Almeras (c_almeras@yahoo.fr)

Franck Bladou (franck.bladou@chu-bordeaux.fr)

Jean-Christophe Bernhard (jean-christophe.bernhard@chu-bordeaux.fr)

Gregoire Robert (gregoire.robert@chu-bordeaux.fr)

Olivier Traxer (olivier.traxer@aphp.fr)

Michel Daudon (michel.daudon@aphp.fr)

Keywords: Morpho-constitutional analysis of urinary stones, flexible ureteroscopy training, endoscopic diagnosis, aetiological lithiasis, LASER fragmentation of stones.

Abbreviations:

1. ESR is **E**ndoscopic **S**tone **R**ecognition,
2. LASER is **L**ight **A**mplification by **S**timulated **E**mission of **R**adiation,
3. FTIR is **F**ourier **T**ransform **I**nfra**R**ed spectroscopy.
4. CCD sensor is **C**harge-**C**oupled **D**evice sensor

ABSTRACT

Objective: To improve endoscopic recognition of the most frequently encountered kidney stone morphologies for a better etiological approach in lithiasis by urologists.

Materials and methods: An expert urologist intra-operatively and prospectively (between June 2015 and June 2018) examined the surface, the section and the nucleus of all encountered kidney stones. Fragmented stones were subsequently analysed by a biologist based on both microscopic morphological (i.e. binocular magnifying glass) and infrared (i.e. FTIR) examinations (microscopists were blinded to the endoscopic data). Morphological criteria were collected and classified for the endoscopic and microscopic studies. The Wilcoxon–Mann–Whitney test was carried out to detect differences between the endoscopic and microscopic diagnoses. A diagnosis for a given urinary stone was considered "confirmed" for a non-statistically significant difference.

Results: A total of 399 urinary stones were included in this study: 51.4% of the stones exhibited only one morphological type while 48.6% were mixed stones (41% had at least two morphologies and 7.6% had three morphologies). The overall matching rate was 81.6%. Diagnostics were confirmed for the following morphologies: whewellite (Ia or Ib), weddellite (IIa or IIb), uric acid (IIIa or IIIb), carbapatite-struvite association (IVb), brushite (IVd).

Conclusions: Our preliminary study demonstrates the feasibility of using endoscopic morphology for the most frequently encountered urinary stones and didactic boards of confirmed endoscopic images are provided. The current study constitutes the first step toward endoscopic stone recognition, which is essential in lithiasis. We provide didactic boards of confirmed endoscopic images which paves the way for automatic computer-aided in-situ recognition.

INTRODUCTION

A morpho-constitutional examination of urinary stones plays an essential role in the aetiological diagnosis [1-5]. The international morpho-constitutional classification of urinary stones includes seven groups denoted by roman numerals (i.e. “I” to “VI”) (Table 1). Each group is associated with a specific crystalline type: I = whewellite, II = weddellite, III = uric acid and urates, IV = calcium and non-calcium phosphates, and V = cystine (group VI other stones). Each group is then divided into several subgroups to differentiate morphologies and aetiologies for a given crystalline type. Five morphological subtypes are encountered in whewellite group I (differentiated by subscripts in the Latin alphabet: Ia to Ie), each one being associated with a specific aetiology. Practically: Ia = excessive concentration of oxalate in the urine induced by diet or default of diuresis, Ic = inherited primary hyperoxaluria, Ie = enteric hyperoxaluria induced by inflammatory bowel disease or by-pass. Interestingly, the most recent lithogenic events (in chronological order) are located on the surface of the stone, whereas less recent events are observable on a section of the stone. The nucleus of the stone, which is the oldest part, corresponds to the initial lithogenic context. Urinary stones are mixed (i.e. include at least two morphologies) in almost half of cases [5].

Daudon and Cloutier emphasised the importance of studying urinary stone morphologies [1, 3, 5] for an aetiological diagnosis of stone disease. A complete examination of the entire stone includes a visual morphological examination of the stone surface, the stone section and the nucleus, as well as a spectrophotometric infrared recognition (FTIR) analysis of crushed stone fragments. However, it is now well established that modern endoscopic treatment of urinary stones relies on LASER fragmentation [6-13]. Fragmentation, whether achieved with "popcorn" [6] or "dusting" modes [7], destroys the morphology of the targeted stone [8]. The morphological examination, which is the first essential diagnostic step, is impossible to redo once the stone is destroyed. Moreover, Keller et al. recently showed the impact of LASER-based dusting on changes in stone composition with significant changes in the infrared spectra (particularly for weddellite, carbapatite, struvite and brushite) [8]. Consequently, a FTIR examination of the stone powder itself does not provide sufficient information to determine correctly the lithogenic stage [1-5]. This finding reinforces the need to observe the morphology of the stone before LASER-induced destruction to preserve an aetiological approach.

The current study constitutes the first step toward endoscopic stone recognition (ESR). We aimed to improve the recognition of the most frequently encountered kidney stone morphologies. Thus, an endoscopic-based examination of unfragmented stones was compared with microscopic observations of laser-fragmented stones, and a concordance study was conducted.

MATERIAL & METHOD

The study adhered to all local regulations and data protection agency recommendations (the National Commission on Informatics and Liberty (CNIL) dictates). Patients have been informed for the use of their data anonymously.

Endoscopic study

An expert urologist (VE, 20 years of experience) intra-operatively and prospectively examined stones between June 2015 and June 2018 using a flexible digital ureterorenoscope (Olympus URF-V CCD sensor). We recall that visual cues that the surgeon has to consider for the estimation of a stone type are summarized in Table 1. The examination included a visual observation of the stone surface first, before LASER fragmentation, then visual observation of the section and the nucleus and after LASER stone section. LASER-based stone section in two parts was performed using the following LASER parameters: frequency = 5 Hz, energy = 1.2–1.4 J, power = 6–7 W, pulse length = short, fibre diameter = 230 or 270 µm [14,15]. That way, it was possible to fragment all types of pure and mixed stones. Once fragmented, the fragments were removed with a Nitinol basket (Zerotip 1.9) through the ureteral access sheat Coloplast Retrace 12/14 or 10/12. An additional fragmentation session was carried out when needed. Macro-fragments including at least one representative copy of the stone surface, the stone section and the nucleus were removed using a nitinol basket for subsequent examination in a dedicated laboratory.

Microscopic study

The fragmented stones were subsequently analysed by a biologist (MD, 40 years of experience) based on both morphological (i.e. binocular magnifying glass) and infrared (i.e.

SPIR) analyses. Similar to the above-mentioned endoscopic analysis, the examination included the surface, the section and the nucleus of each stone.

Observations

The urinary stones were classified according to microscopic morphological instructions given by Daudon et al. in [1]. We collected the following eight observations for all urinary stones in the endoscopic and microscopic studies.

- Three observations about surface morphology referred to as “majority” (for the most visible morphology on the surface of the stone), “secondary” (for potentially secondary visible morphology) and “minority” (for another potentially visible morphology).
- Three observations about the inner structure: “central” (for the morphology visible in the centre of the stone), “peripheral” (for the morphology visible on the periphery of the stone) and “intermediate” (for the morphology in between).
- Two observations about the nucleus: “majority” (for the most visible morphology in the nucleus of the stone) and “minority” (for another potentially visible morphology).

Concordance between the endoscopic- and microscopic-based observations

All data were collected into a single Excel spreadsheet that was retrospectively analysed using Matlab software (MathWorks, Inc., Natick, MA, USA).

We selected a subset of urinary stones for which “Ia” or “Ib” morphologies were encountered in any microscopic-based observation. Among these, urinary stones for which the “Ia” or “Ib” morphologies were encountered in any endoscopic-based observation were listed and referred to as a “good match”. The total number of urinary stones with a “good match” was calculated and recorded. The Wilcoxon-Mann-Whitney test was carried out to determine whether the differences between endoscopic and microscopic diagnoses were significant. A significance threshold of $p = 0.05$ was used. A diagnosis for a given urinary stone was considered “confirmed” for a non- significant difference between the endoscopic and microscopic examinations ($p > 0.05$). In such a case, the area under the ROC curve (AUROC), sensitivity, specificity, positive predictive value (PPV) and negative predictive value (NPV)

were calculated (considering the presence of a given morphology in the microscopic study as a “positive case”).

RESULTS

Demographic characteristics

In total, 399 urinary stones were included in this retrospective study. Among them, 48.6% were mixed stones (41% had at least two morphologies and 7.6% had three morphologies). Our cohort was composed of 63% calcium oxalate stones (group I whewellite + group II weddellite), 20% phosphate stones (group IV: carbapatite, brushite and struvite), 15% uric acid and urate stones (group III), 0.2% cystine (group V) and 1.8% of other stones (group VI).

Typical images obtained for each of the six urinary stone groups are shown in Figures 1 to 9 respectively. Endoscopic- and microscopic-based observations of the stone surface and sections are reported, together with corresponding aetiological conditions.

Stone morphologies analysed

We identified 16 morphologies distributed over the following groups:

- For whewellite group I: Ia, Ib, Id and Ie
- For weddellite group II: IIa and IIb
- For the uric acid and urate group III: IIIa and IIIb
- For the calcium and non-calcium phosphate group IV: IVa1 and IVa2 (carbapatite), IVb (carbapatite and struvite), IVc (struvite), IVd (brushite).
- For the cystine group V: Va
- For the group VI aggregating other stones (protein matrices +/- whewellite): VIa and VIb

For this study, we grouped the following morphologies that had similar aetiologies: Ia and Ib, IIa and IIb, IIIa and IIIb, Va and Vb and VIa and VIb.

Concordance between the endoscopic- and microscopic-based observations

Table 2 summarises the concordance between our endoscopic- and microscopic-based observations.

Morphologies validated by the microscopic and endoscopic examinations

Diagnoses were confirmed for the following morphologies: whewellite (Ia or Ib: concordance = 85%, n = 205 ; Id: concordance = 92%, n = 12 ; Ie: concordance = 80%, n = 5), weddellite (IIa or IIb: concordance = 85%, n = 178), uric acid (IIIa or IIIb: concordance = 91% n = 64), carbapatite-struvite association (IVb: concordance = 50%, n = 10), brushite (IVd: concordance = 65%, n = 23). Several other pure stone morphologies depicted good matching, although just below the significance threshold of 0.05, such as carbapatite (IVa1, concordance = 81%, n = 176). Other pure stone morphologies depicted excellent matching but insufficient number of cases, such as cystine (Va: concordance = 100%, n = 1).

DISCUSSION

Our study consisted of endoscopic recognition of the morphological elements constituting urinary stones before LASER stone destruction. ESR allows the morphological identification of an entire stone and is thus essential in lithiasis. While the main objective of ESR is to identify a stone type, it also provides examinations of the anatomy of the excretory pathway as well as the renal papillae. Flexible ureteroscopy is thus a great diagnostic and therapeutic candidate in lithiasis. We offer didactic boards to help with endoscopic recognition comprised of reference images and descriptions (surface, section and nucleus), and the lithogenic mechanisms and aetiologies associated with each morphology (Figures 1–6).

It must be reported that a learning curve is needed to acquire the ESR skill which may limit its translation to practical use. In the current study, the urologist (VE) had, first of all, to learn the classification of the different types of stone surface, section and nuclei using the microscopic images provided by Daudon and al. [1,3,5]. Subsequently, he had to acquire the ability to recognize such types of stone surface, section and nuclei on endoscopic images, based on the learned microscopic images and associated descriptions. Along this line, one goal of our concordance study is to reduce possible subjectivity in ESR and urologist bias by history. To make easier the ESR for urologist, we propose didactic boards of confirmed endoscopic images for the most frequently encountered urinary stones on a daily practice. This follows the work of Bergot et al. which showed that ESR teaching of junior urologists allows them to acquire the skill to recognize the most frequently encountered stones quickly [17]. On the other hand, a computer-assisted approach delivers reproducible results and minimises operator dependency, as visual interpretation of stone images lacks a learning curve when the process is automated. It is therefore promising to train artificial intelligence algorithms with our confirmed endoscopic images. Black et al. have recently shown that artificial intelligence (deep learning) applied to in vitro surface and section images of stones represents a great asset for the automatic recognition of whewellite, weddellite, uric acid, brushite and struvite stones [21]. Such algorithms may be able to do tests with various pre-defined score and error levels. Combined with our confirmed endoscopic images, deep neural networks, such as convolutional neural networks (CNN), which are able to process efficiently a high number of specific images and videos, are good candidates for automatic ESR.

In our study, the SPIR examination detected 12 struvite cases that were not described using morphological analyses. The combination of morphological and SPIR examinations improved the diagnostic concordance of urolithiasis [1-4]. Our findings of the epidemiological distribution of the different crystalline types as well as the rate of pure/mixed stones are in line with already published results [16]. Therefore, our cohort is representative of the stone distribution that any urologist might encounter. Our study confirmed the following six morphological types: Ia or Ib, IIa or IIb, IIIa or IIIb, IVa, IVb and IVd. These six morphological types cover 95% of the most common pure stones that urologists encounter in its practice daily [5].

Our study showed that recognising the main morphological surface criteria is easier than the other stages of the analysis (i.e. section and nucleus). This result is crucial because the majority of the surface area of a urinary stone represents recent lithogenesis. Its destruction by a LASER *de facto* leads to a loss of aetiological information.

The enthusiasm of urologists for the LASER spraying of calculations in the “dusting” mode and the upcoming arrival of a new generation of very high frequency “super Thulium fibered” LASER [18, 19] will positively affect the success of interventions to minimise the rate of residual fragments and improve results without fragments.

However, the urologist should not forget that the morpho-constitutional examination of a urinary stone, which is currently the only solution for observing the entire stone, is as important as the pathological examination of a surgical specimen for the therapeutic strategy of onco-urology cases.

Despite the variety of compositions and morphologies observed in urinary calculi, about 90% are composed of a limited number of crystalline species and morphological characteristics that are easily recognised through an endoscopic examination. The morpho-constitutional classification of urinary stones previously published is particularly suitable for this purpose. Endoscopic examination of 399 stones revealed good concordance between endoscopic and microscopic typing of the stones. For example, concordance of the results was observed in 86.1% of type I stones, 85% of type II stones, 91% of type III stones and 79% of type IV stones made of calcium phosphate. Within stone types, it was possible to identify with good agreement specific subtypes related to a more accurate aetiological diagnosis, such as

subtype Ia or Ib, which is mainly related to dietary hyperoxaluria due to oxalate-rich food intake or low diuresis, while subtype Ie is related to enteric hyperoxaluria. Subtype Id stones suggest stasis and anatomical confinement related to urological anomalies. The presence of a thin greyish layer on the surface of a type Ia stone is a marker for dietary hyperoxaluria in most cases. ESR may be more critical when mixtures of phosphates are present, as suggested by differences in concordance among the various subtypes. As shown in Table 2, concordance was high (about 80%) for subtype IVa1 and IVb stones. In contrast, concordance was lower (65%) for subtype IVd, which is a marker for brushite-containing stones. Concordance was significantly better when brushite was the main component of the stone, reaching 77.8% of cases. However, the concordance between the endoscopic and microscopic examinations was only 21% for IVa2 stones, which are mainly composed of carbapatite. Two reasons could explain this low concordance. First, subtype IVa2 is uncommon. Second, some morphological characteristics of these stones, such as the presence of tiny cracks within the structure, are reinforced by drying the stone before the microscopic examination, and thus could be less visible during the endoscopic analysis. Training based on an examination of a larger number of samples would improve the concordance for the stone types providing poor agreement between the endoscopic and microscopic examinations. Notably, the global concordance level was 81.6% in this first study.

As Almeras et al described a higher incidence of IVa2 stones when intra papillary cristallization occured and others descriptions correlated to different lithogenesis mechanisms, the description of papillary abnormalities during flexible ureteroscopies would certainly add a diagnostic value to this endoscopic stone recognition [20].

It should be emphasised that it is essential to record the traceability of the morphology of the surface, the section and the nucleus of a urinary stone. The urologist must archive all images to allow retrospective expertise, if necessary, by a biologist, an expert urologist or machine learning.

CONCLUSION

This study provided a 81.6% concordance between endoscopic and microscopic urine stone characterisations. We created didactic boards of confirmed endoscopic images for the most

frequently encountered urinary pure stones, including whewellite (Ia or Ib, Id, Ie), weddellite (IIa or IIb), uric acid (IIIa or IIIb), carbapatite (IVa or IVb), brushite (IVd) and cystine (Va or Vb). These boards can be used by urologists to learn how to recognise stones *in-situ* using an endoscopic examination before they are destroyed. Thereby, urologists must be more involved in the aetiological diagnosis, as well as in the therapeutic nephrolithiasis strategy, to maintain an essential role in the decision tree of urinary stone management.

This first series of endoscopic images will be supplemented by more stone images in future studies to increase the number of examples of rarer urinary stones. This task is already in progress at our institution and will rely on the epidemiological distribution of the occurrence of urinary stones to obtain a sufficiently large population for an opposable statistical approach.

Accurate recognition of the most frequently encountered kidney stone morphologies allows for the development of an endoscopic stone image data base designed for automatic computer-aided *in-situ* recognition.

REFERENCES

1. Daudon M, CA Bader, Jungers P. Urinary Calculi: Review of classification methods and correlations with etiology. Scanning Microsc. 1993 ; 7 (3):1081-104.
2. Daudon M, Jungers P, Bazin D, et al. Recurrence rates of urinary calculi according to stone composition and morphology. Urolithiasis. 2018;46(5):459-470. https://doi:10.1007/s00240-018-1043-0.
3. Cloutier J, Villa L, Traxer O, et al. Kidney stone analysis: "Give me your stone, I will tell you who you are!". World J Urol. 2015 ;33(2):157-69. https://doi: 10.1016/j.eururo.2016.03.035.
4. Estrade V, Daudon M, Méria P, et al. Why should urologist recognize urinary stone and how? The basis of endoscopic recognition. Prog Urol – FMC 2017;27:F26—35. https://doi.org/10.1016/j.fpurol.2017.03.002.
5. Daudon M, Dessombz A, Frochot V, et al. Comprehensive morpho-constitutional analysis of urinary stone improves etiological diagnosis and therapeutic strategy of nephrolithiasis. Comptes Rendus Chimie. 2016 ; 19:1470-1491. http://dx.doi.org/10.1016/j.crci.2016.05.008.
6. Emiliani E, Talso M, Cho SY, et al. Optimal Settings for the Noncontact Holmium:YAG Stone Fragmentation Popcorn Technique. J Urol. 2017 ;198(3):702-706. https://doi: 10.1016/j.juro.2017.02.3371.
7. Doizi S, Keller EX, De Coninck V, et al. Dusting technique for lithotripsy: what does it mean?. Nat Rev Urol. 2018 ;15(11):653-654. https://doi: 10.1038/s41585-018-0042-9.
8. Keller EX, De Coninck V, Doizi S, et al. Thulium fiber laser: ready to dust all urinary stone composition types?. World J Urol. 2020; 3. https://doi.org/10.1007/s00345-020-03217-9.
9. Doizi S, Raynal G, Traxer O. Evolution of the stone treatment over 30 years in a French academic institution. Prog Urol. 2015 ; 25 (9):543-8. https://doi:10.1016/j.purol.2015.05.002.
10. Carpentier X, Meria P, K Bensalah, et al. Management of Adult's Renal and Ureteral Stones. Update of the Lithiasis Committee of the French Association of Urology (CLAFU). General Considerations . Prog Urol. 2014 ;24 (5):319-26. https://doi: 10.1016/j.purol.2013.08.315.
11. Chabannes E, Bensalah K, Carpentier X, et al. Management of adult's renal and ureteral stones. Update of the Lithiasis Committee of the French Association of Urology (CLAFU). General considerations. Prog Urol. 2013 ;23(16):1389-1399. https://doi: 10.1016/j.purol.2013.08.315.
12. Estrade V, Bensalah K, Bringer JP, et al. Place of the flexible ureterorenoscopy first choice for the treatment of kidney stones. Survey results practice committee of the AFU lithiasis completed in 2011. Prog Urol. 2013;23(1):22-28. : 10. https://doi:1016/j.purol.2012.09.003.

13. Raynal G, Merlet B, Traxer O. In-hospital stays for urolithiasis: Analysis of French national data. Prog Urol . 2011 ; 21 (7) :459-62. https://doi: 10.1016/j.purol.2011.02.002.

14. Traxer O, Lechevallier E, Saussine C. Flexible ureteroscopy with Holmium laser: technical aspects. Prog Urol 2008 ;18(12):929-37. https://doi: 10.1016/j.purol.2008.09.034.

15. Traxer O, Lechevallier E, Saussine C. Flexible ureteroscopy with Holmium laser: the tools. Prog Urol 2008 ;18(12):917-28. https://doi: 10.1016/j.purol.2008.09.038.

16. Daudon M, Traxer O, Lechevallier E, et al. Epidemiology of urolithiasis. Prog Urol. 2008 ;18(12):802-814. https://doi: 10.1016/j.purol.2008.09.029.

17. Bergot C, Robert G., Bernhard JC, et al. The basis of endoscopic stones recognition, a prospective monocentric study. Prog Urol. 2019 ;29(6):312-317. https://doi: 10.1016/j.purol.2019.04.002.

18. Andreeva V, Vinarov A, Yaroslavsky I, et al. Preclinical comparison of superpulse thulium fiber laser and a holmium:YAG laser for lithotripsy. World J Urol 2020 ;38(2):497-503. https://doi: 10.1007/s00345-019-02785-9.

19. Traxer O, Keller EX. Thulium fiber laser: the new player for kidney stone treatment? A comparison with Holmium:YAG laser. World J Urol. 2020 ;38(8):1883-1894. https://doi: 10.1007/s00345-019-02654-5.

20. Almeras C, Daudon M, Estrade V et al. Classification of the renal papillary abnormalities by flexible ureteroscopy: evaluation of the 2016 version and update. World J Urol. 2020 ;19. https://doi: 10.1007/s00345-020-03149-4

21. Black KM, Law H, Aldoukhi A, et al. Deep learning computer vision algorithm for detecting kidney stone composition. BJU Int 2020 ;125(6):920-924. https://doi: 10.1111/bju.15035.

TABLE LEGENDS

Table 1: Morpho-constitutional classification of urinary stones.

Type	Surface	Section
Ia	Smooth or mammillary, dark-brown surface. Frequent papillary umbilication with a piece of Randall's plaque	Section showing compact concentric layers with a radiating organization starting from a nucleus (often a Randall's plaque)
Ib	Mammillary, rough surface. Color : brown to dark-brown,	Unorganized section. Absence of an umbilication
Id	Very smooth surface, beige or pale brown in color	Compact section showing thin concentric layers without radiations
Ic	Pale brown-yellowish budding surface (without any umbilication)	Loose, unorganized section. Light color
Ie	Locally budding, mamillary or rough surface. Heterogeneous color from brown-yellow pale to dark brown	Heterogeneous structure, with a mixture of poorly organized brown-yellow pale areas and of locally concentric dark brown layers with radiating organization.
IIa	Yellow or light-brown prickly, spiculated surface due to presence of aggregated bipyramidal crystals with sharp angles and edges	Loose radial crystallization. Color : pale brown-yellow
IIb	Yellowish or light-brown surface with smooth, long bipyramidal crystals, thus resembling small desert roses	Compact poorly organized crystalline section. Color : pale brown-yellow
IIc	Rough grey-beige to pale brown surface,	Diffuse concentric structure at the periphery
IIIa	Homogeneous smooth surface. Color : typically orange	Concentric layers with a radiating organization around a well-defined nucleus. Color : ochre to orange
IIIb	Rough and porous surface with a heterogeneous, beige to orange-red color	Poorly organized, porous structure. Color : Ochre to orange
IIIc	Rough and locally porous beige or greyish surface.	Unorganized porous section of same color as surface
IIId	Heterogeneous, embossed, rough and porous surface with a greyish to dark-brown color.	Alternative thick, brown and thin, beige layers with small porous zones.
IVa1	Whitish, rough homogenous surface.	Poorly organized structure, with loose concentric layers of same color as the surface.
IVa2	Very peculiar morphology characterized by a yellow-brown, smooth surface with a glazed appearance and small cracks	Section showing irregularly arranged thin whitish and thick yellow-brown concentric layers.

IVb	Heterogeneous surface, both embossed and rough. Heterogeneous color from whitish to dark brown.	Alternate thick whitish and thin brown-yellow layers.
IVc	Aggregates of large crystals with blunt angles and edges. Color : Whitish color.	Diffuse, loose radial crystallization. Whitish color.
IVd	Large rod-shaped crystals thereafter evolving toward slightly rough surface or resembling cabbage. Color : whitish or beige.	Radial crystallization with locally concentric layers. Color : whitish to beige.
Va	Homogeneous, bumpy or rough, surface. Waxy aspect. Color: light brown yellow.	Diffuse radial organization or unorganized section. Color: light brown-yellow.
Vb	Homogeneous smooth or finely rough surface, Color: whitish to pale beige.	Heterogenous structure made of finely concentric microcrystalline beige organization in periphery around a compact, crystalline unorganized light brown-yellow core.
VIa	Soft matrices, light-brown in color in contrast with other types of protein-rich calculi.	Unorganized structure. Color: light brown.

Table 2. Match results between endoscopic and microscopic studies. *p*-values denoted by "/" corresponds to data that are insufficiently populated for statistical comparison. Non-significant differences between endoscopy and microscopy analysis are denoted by "NS". AUC: area under the ROC curve; PPV: positive predictive value; NPV: negative predictive value; FPR: false predictive rate; FNR: false negative rate. AUROC, Sensitivity, Specificity, PPV, NPV, FPR and FNR are reported only for non-significant differences between endoscopy and microscopy findings.

Kidney Type	Good match # (%)	Bad match # (%)	Total #	*p*	AUC	Sensitivity (%)	Specificity (%)	PPV (%)	NPV (%)	FPR (%)	FNR (%)
Ia or Ib	175 (85%)	30 (15%)	205	NS	0.87	85%	88%	89%	85%	12%	15%
Ia active	7 (100%)	0 (0%)	7	/	/	/	/	/	/	/	/
Id	12 (92%)	1 (8%)	13	NS	0.96	92%	99%	80%	100%	1%	8%
Ie	4 (80%)	1 (20%)	5	NS	0.90	80%	100%	100%	100%	0%	20%
IIa or IIb	151 (85%)	27 (15%)	178	NS	0.87	85%	88%	86%	88%	12%	15%
IIIa or IIIb	58 (91%)	6 (9%)	64	NS	0.95	91%	99%	94%	98%	1%	9%
IIIc	0 (0%)	3 (100%)	3	/	/	/	/	/	/	/	/
IVa1	142 (81%)	34 (19%)	176	0.03	0.86	81%	91%	88%	85%	9%	19%
IVa2	3 (21%)	11 (79%)	14	0.02	0.6	21%	99%	43%	97%	1%	79%
IVb	5 (50%)	5 (50%)	10	NS	0.74	50%	98%	45%	99%	2%	50%
IVc	9 (75%)	3 (25%)	12	0.001	0.86	75%	96%	39%	99%	4%	25%
IVd	15 (65%)	8 (45%)	23	NS	0.82	65%	99%	83%	98%	1%	35%
Va	7 (100%)	0 (0%)	7	/	/	/	/	/	/	/	/
VIa or VIb	2 (33%)	4 (67%)	6	NS	0.67	33%	100%	100%	99%	0%	67%
Total	**590 (82%)**	**133 (18%)**	**723**	-	-	-	-	-	-	-	-

Figure N°1 : Pure stone type **Ia or Ib**

	Pure Stone type **Ia or Ib**-: Component : whewellite answers=205 : good match=85% *p*=NS	
Descriptive anatomy of stone morphology	**Microscopic reference images**	**Endoscopic images**
Surface : ***Ia :***Mamillary dark-brown surface. Frequent umbilication and Randall'splaque indicative of papillary origin ***Ib :*** brown to dark-brown, mamillary, rough surface	*Ia* 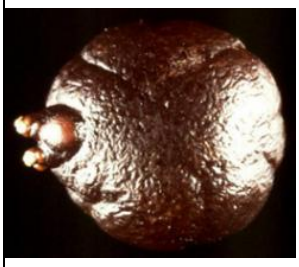 *Ib* 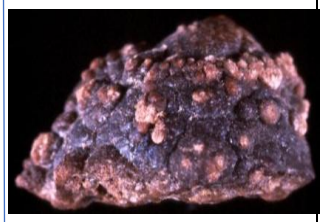	*Ia*  *Ib* 
Section : ***Ia :*** Section made of compact concentric layers with radiating organization starting from a nucleus. Color: dark brown ***Ib :***unorganized section and they never exhibit an umbilication	*Ia* 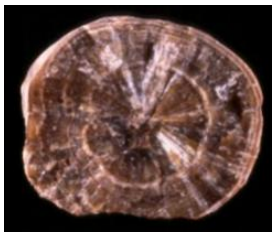 *Ib* 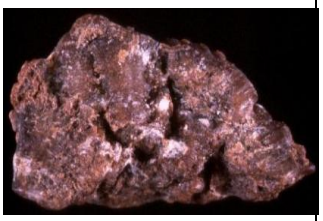	*Ia* 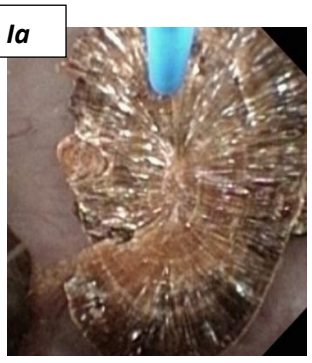 *Ib* 

Common Etiology :	*Dietary hyperoxaluria, low diuresis (high oxalate concentration), Randall's plaque*

Figure N°2 : Pure stone type **Id**

	Pure Stone type **Id** : Component <u>whewellite</u> answers **=13 :** good match 92% *p*=NS	
Descriptive anatomy of stone morphology	**Microscopic reference images**	**Endoscopic images**
Surface : Very smooth surface, beige or pale brown in color		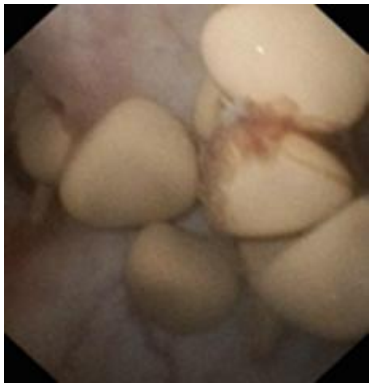
Section : Showing compact thin concentric layers without radiations. Color: beige or pale brown		
Common Etiology :	*Malformative uropathy, stasis and confined multiple stones*	

Figure N°3 : Pure stone type **Ie**

	Pure Stone type **Ie** : Component <u>whewellite</u> answers **= 5 :** good match 80% *p*=NS	
Descriptive anatomy of stone morphology	**Microscopic reference images**	**Endoscopic images**
Surface : exhibit a locally budding, mamillary or rough brown-yellow pale surface,	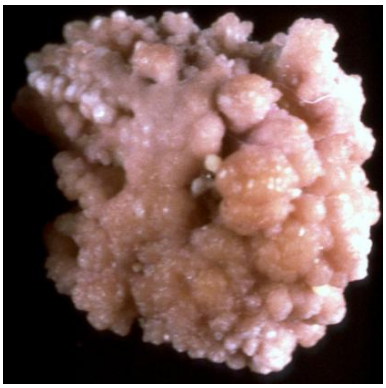	
Section : heterogeneous structure, with a mixture of poorly organized brown-yellow pale areas and of locally concentric dark brown layers with radiating organization	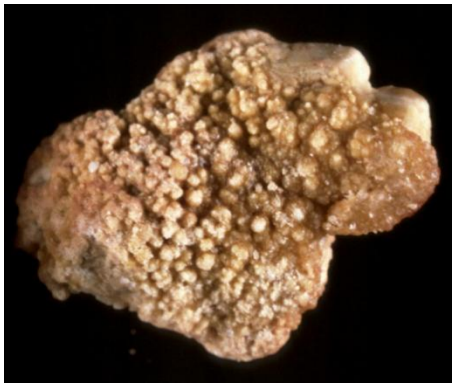	
Common Etiology :	*Enteric hyperoxaluria, inflammatory bowel diseases (Chron desease), ileal resections, chronic pancreatis.*	

Figure N°4 : Pure stone type **IIa or IIb**

	Pure Stone type **IIa** or **IIb**: Component weddellite answers =178 : good match =85% *p*=NS	
Descriptive anatomy of stone morphology	**Microscopic reference images**	**Endoscopic images**
Surface : ***IIa***: Yellowish or light-brown prickly, spiculated surface due to presence of aggregated bipyramidal crystals with sharp angles and edges or ***IIb :*** They have a yellow or light-brown surface with smooth, long bipyramidal crystals, thus resembling small „desert roses“,	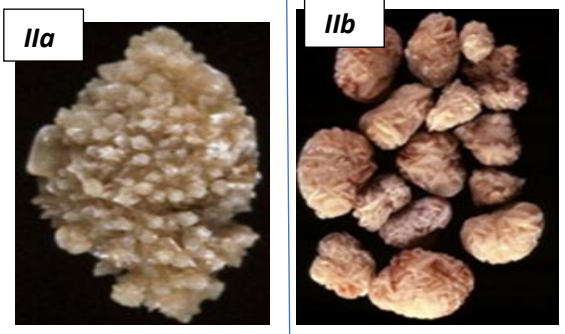	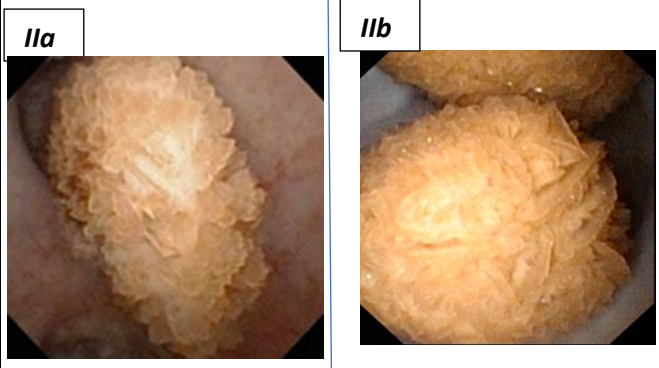

Section : ***IIa:*** Section showing loose radial crystallization. Color: yellowish to light brown ***IIb :*** compact poorly organized crystalline section	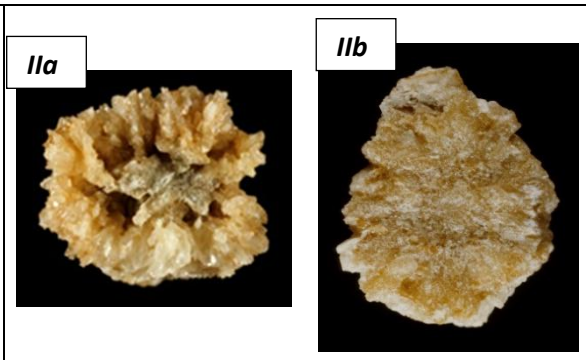	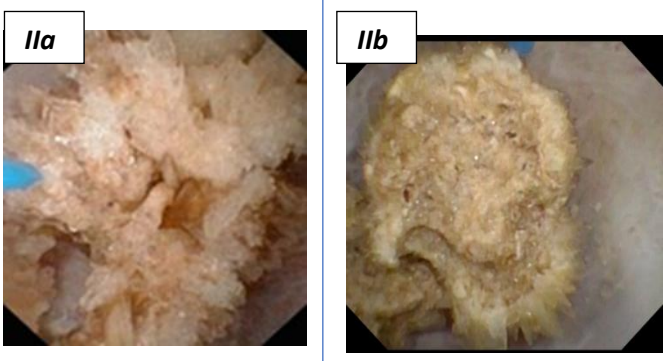
Common Etiology :	***IIa*** *:Hypercalciuria,whatever its origin, high molar ratio calcium/citrate* ***IIb*** *:Hypercalciuria ± hyperoxaluria ± hypocitraturia, Stasis, low diuresis*	

Figure N°5 : Pure stone type **IIIa or IIIb**

	Pure Stone type **IIIa** and **IIIb**: Component uric acid anhydrous answers= 64 : good match =91% *p*=NS	
Descriptive anatomy of stone morphology	**Microscopic reference images**	**Endoscopic images**
Surface : ***IIIa:*** Homogenous smooth surface. Color: typically, orange ***IIIb :*** rough and porous surface with a heterogeneous, beige to orange, color and an orange-red		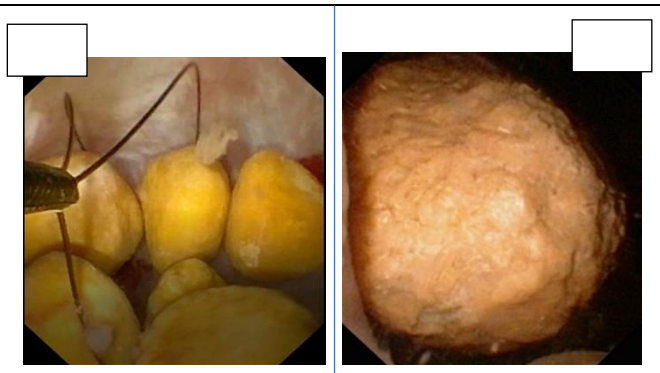
Section : ***IIIa :*** Compact concentric layers with a radiating organization around a well-defined nucleus. Color: ocher to orange ***IIIb :*** with a poorly organized, porous structure.		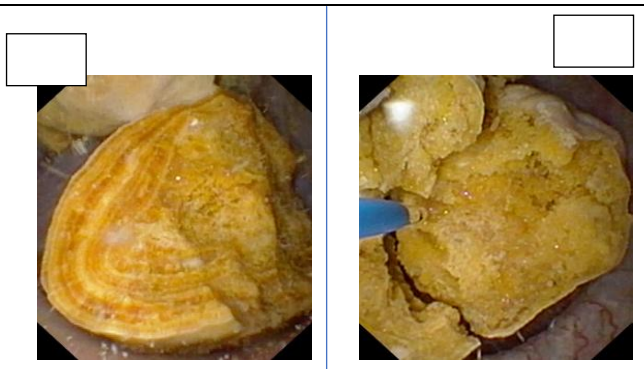

Common Etiology :	***IIIa :****Low urine pH, stasis prostate hypertrophy, metabolic syndrome, ammoniagenesis defect* ***IIIb :****Insulin resistance, metabolic syndrome, type 2 diabetes, ammoniagenesis defect, low urine pH*

Figure N°6 : Pure stone type **IVa**

	Pure Stone type **IVa:** Component carbapatite answers=176 good match = 81% *p*=NS	
Descriptive anatomy of stone morphology	**Microscopic reference images**	**Endoscopic images**
Surface : exhibit a whitish, rough homogeneous surface	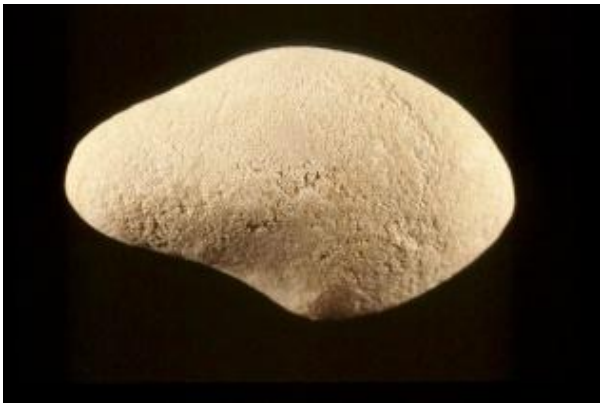	

Section : section shows a poorly organized structure, with loose concentric layers of same color as the surface		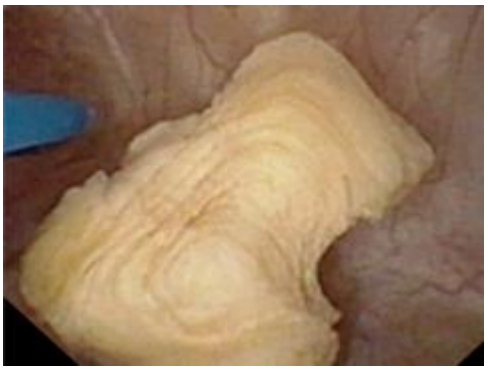
Common Etiology :	*Hypercalciuria, urinary tract infection.* *Etiology may be oriented by the presence of other crystalline species and by the carbonatation rate of carbonated calcium phosphates*	

Figure N°7 : Pure stone type **IVb**

	Pure Stone type **IVb:** Component carbapatite answers=10 good match = 50% *p*=NS	
Descriptive anatomy of stone morphology	**Microscopic reference images**	**Endoscopic images**
Surface : heterogeneous surface, both embossed and rough, of clear to dark brown color.		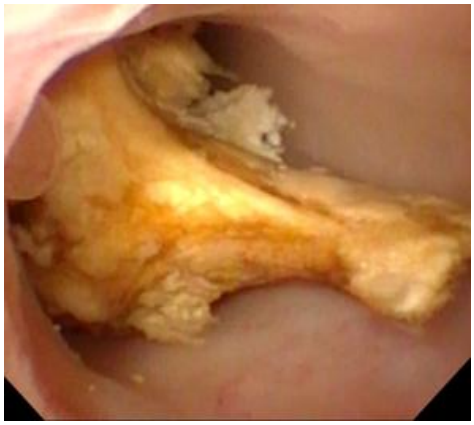
Section : section is made of alternate thick whitish and thin brown-yellow layers		

Common Etiology :	*Urinary tract infection, Hypercalciuria, primary hyperparathyroidism*

Figure N°8 : Pure stone type **IVd**

	Pure Stone type **IVd :** Component brushite n= 22 : good match = 59% *p*=NS	
Descriptive anatomy of stone morphology	**Microscopic reference images**	**Endoscopic images**
Surface : Large rod-shaped crystals thereafter evolving toward slightly rough or resembling cabbage, whitish or beige surface		

Section : Compact radial crystallization with locally concentric layers		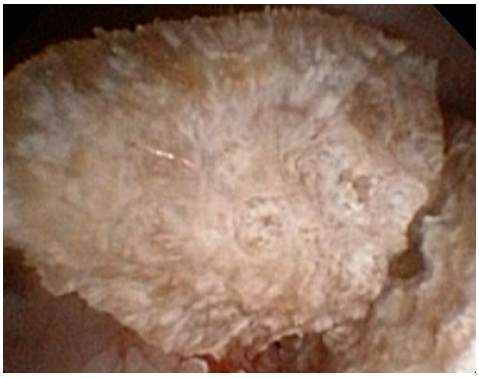
Common Etiology :	*Hypercalciuria, primary hyperparathyroidism, phosphate leak, medullary sponge kidney*	

Figure N°9 : Pure stone type **Va**

	Pure Stone type **Va :** Component <u>cystine</u> n= 7 : good match = 100% *p*=NS	
Descriptive anatomy of stone morphology	**Microscopic reference images**	**Endoscopic images**
Surface : Homogeneous, bumpy or rough, waxy in color homogeneous brown-light yellow.		

Section : Diffuse or unorganized radial, light brown-yellow		
Common Etiology :	*Cystinuria*	